Organic & Biomolecular Chemistry

Concerning The Mechanism of Iodine(III)-Mediated Oxidative Dearomatization of Phenols

SCHOLARONE™
Manuscripts

Journal Name

ARTICLE

Concerning The Mechanism of Iodine(III)-Mediated Oxidative Dearomatization of Phenols

Andrew M. Harned*[a]

The iodine(III)-mediated oxidative dearomatization of phenols has proven to be a general method for the preparation of cyclohexadienones. While this is a widely used reaction, there is still a great deal of uncertainty regarding the mechanistic pathway followed by these reactions. In part, this is due to the highly unstable nature of many of the key intermediates, which makes their direct detection extremely difficult. In order to gain some insight into these mechanistic questions, DFT calculations [M06-2X/6–31+G(d) for C, H, and O and LANL2DZdp for iodine] were used to evaluate the two most commonly proposed reaction mechanisms. These results show that unimolecular fragmentation of an oxygen-bound intermediate to give a phenoxenium ion (TS1) is preferred over direct addition of the nucleophile to the aromatic ring of the activated phenol (TS3). In addition, results are presented that suggest, protonation and/or hydrogen bonding may play a key role in lowering the energy of the unimolecular fragmentation pathway.

Introduction

Over the last three decades, there has been a great deal of interest in developing the chemistry of organoiodine(III) compounds (λ^3-iodanes).[1] One of the more common reaction classes involving λ^3-iodanes is the oxidative dearomatization of phenols (Figure 1A).[2] These two-electron oxidations result in the addition of a nucleophile to the aromatic ring of the phenol and the formation of either a 1,3-cyclohexadienone (1) or a 2,5-cyclohexadienone (2). While the overall behavior of the reaction outlined in Figure 1A is generally well understood, the mechanism of this process remains the subject of debate.

Two mechanisms, illustrated in Figure 1B using water as the nucleophile, are commonly proposed for oxidative dearomatization reactions carried out with $PhI(O_2CCH_3)_2$. Both mechanisms require ligand exchange[3] between the phenol and iodine(III) carboxylate to give aryl-λ^3-iodane 3.[4] The first involves direct redox fragmentation of λ^3-iodane 3 (TS1) to give phenoxenium ion 4, the subsequent trapping of which gives rise to dienone 6. The second pathway involves nucleophilic attack on the aromatic ring as shown by TS3. This results in oxidation of the phenoxyl group, reduction of the iodine(III) center, and formation of dienone 6.

Although practitioners have adopted these pathways to rationalize the observed reactivity, we are unaware of a detailed mechanistic study of oxidative dearomatization reactions.[5] This is understandable as the rapid nature of these reactions and the necessity of an initial ligand exchange complicates traditional kinetic analysis. Furthermore, the

highly unstable nature of the relevant intermediates makes their spectroscopic detection and identification challenging.[6,7]
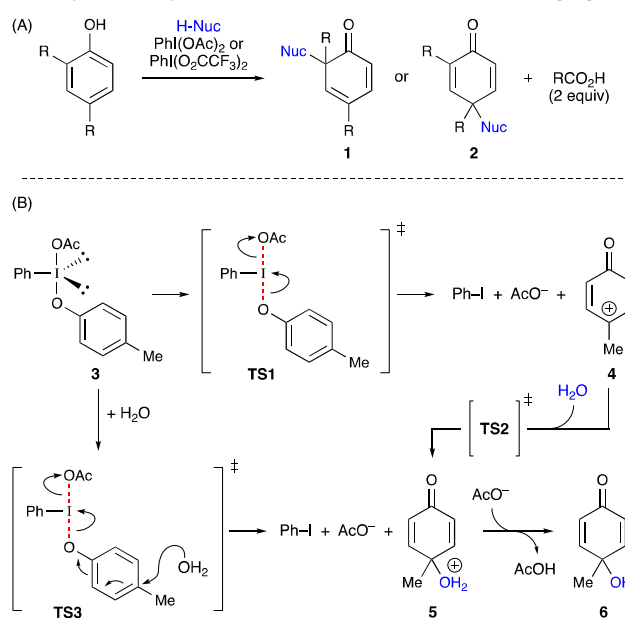

Figure 1. Postulated mechanisms for the iodine(III)-mediated oxidation of phenols.

Having a better understanding of the mechanism of iodine(III)-mediated oxidative dearomatization reactions is needed in order to design aryl iodide catalysts with improved reactivity, and is critically important[8] for the design of new chiral aryl iodide catalysts[9,10] with improved enantioselectivity. With this goal in mind, we decided to perform a computational study[11] (see Experimental Section for details) of the two pathways in the hope that one would emerge as being more

a. Texas Tech University, Department of Chemistry & Biochemistry, 1204 Boston Ave., Lubbock, TX, 79409-1061, United States, Email: andrew.harned@ttu.edu
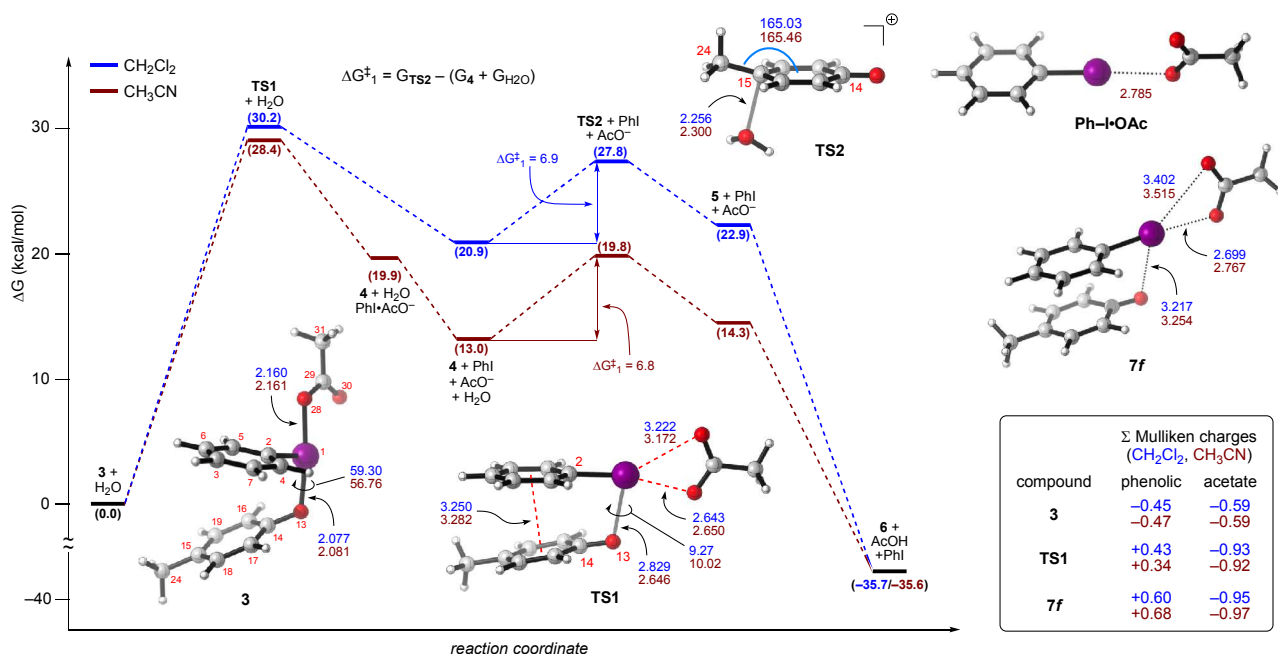
ARTICLE

Figure 2. Energy profile for the reaction of **3** with water using a CH_2Cl_2 (blue) or CH_3CN (maroon) solvation model. The numbers in parentheses are relative free energies (kcal/mol) for the listed compounds. All computed structures shown are with CH_3CN solvation. Structures in CH_2Cl_2 can be found in the supporting information. The indicated centroid and atomic distances are in angstroms. The indicated bond angles and dihedral angles are in degrees. See the supporting information for a complete list of partial charges.

energetically favourable. The results of this study are presented herein.

Results and Discussion

We decided to use water as a simple nucleophile to probe the two decomposition pathways of aryl-λ^3-iodane **3** (Scheme 1B). In order to account for solvation effects, a solvation model for CH_2Cl_2 (a lower polarity solvent) and CH_3CN (a polar, non-nucleophilic solvent) were used. Both solvents are commonly used in oxidative dearomatization reactions.

It is worth noting that Kita has found that oxidative dearomatizations and biaryl couplings of phenol *ethers* and other electron rich aromatics can proceed through radical cation intermediates.[12] Radical mechanisms were not considered here for two reasons. First, the conditions needed to form the requisite radical cation intermediate *require* the use of $PhI(O_2CCF_3)_2$ and either a fluoroalcohol solvent (2,2,2-trifluoroethanol or 1,1,1,3,3,3-hexafluoro-2-propnaol) or an appropriate Lewis acid additive (e.g., $BF_3\bullet OEt_2$ or TMSOTf).[12c] Switching the solvent to either CH_3CN or CH_2Cl_2 has been shown to be deleterious to achieving the radical-based mechanism.[12a] Secondly, during their studies aimed at synthesizing diazonamide A, Harran and co-workers found that an oxidative cyclization of a phenolic substrate performed using $PhI(O_2CCH_3)_2$ afforded a by-product that was not observed when electrochemical (anodic) conditions were employed.[13] This results suggests that the reaction of a phenol with $PhI(O_2CCH_3)_2$ follows a two-electron pathway, rather than a radical pathway.

Investigating the unimolecular decomposition pathway

The calculated energy profile for the reaction proceeding through **TS1** is shown in Figure 2. Overall, lower energies were encountered with the CH_3CN solvation model than with CH_2Cl_2. This is not surprising considering the polar nature of the intermediates generated by these reactions (i.e., **4**, **5**, acetate). **TS1** was found to be ~30 kcal/mol higher in energy than λ^3-iodane **3**. The transition state (**TS2**) for the addition of water to phenoxenium ion **4** was also located. Similar phenoxenium ions, generated by laser flash photolysis, have lifetimes between 3 and 170 ns in water,[7] so it is not surprising that this barrier was quite small (~7 kcal/mol). Although phenoxenium ion **4** and protonated quinol **5** are both higher in energy than λ^3-iodane **3**, this energy cost is mitigated by a presumably rapid deprotonation[14] of **5** by acetate (or other general base). This is evidenced by the precipitous free energy drop upon formation of quinol **6**.

The calculated structure of **TS1**, along with selected measurements, is given in Figure 2. In order to achieve this geometry a rotation about the phenolic O–I bond in λ^3-iodane **3** must occur. This is evidenced by the change in the C2–I–O13–C14 torsion. In **TS1** (10.02° in CH_3CN; 9.27° in CH_2Cl_2) this angle is more acute than it is in **3** (56.76° in CH_3CN; 59.30° in CH_2Cl_2). In addition to rotation of the phenolic O–I bond, the C2–I–OAc angle experiences a large distortion. This is likely related to the development of a σ-hole[15] on the C–I axis as the iodine is being reduced and, consequently, a halogen bond[16] (e.g., **Ph–I•OAc**)[17] between the iodine and the acetate leaving group. The net effect of these structural changes is that the substrate ring slips beneath the aryl iodide ring in **TS1**. This orientation may allow for some stabilization of the developing phenoxenium ion through noncovalent (e.g., cation–π or dispersion)[18,19,20] interactions with the aryl iodide. The centroid-to-centroid distance (~3.25 Å) between the two rings
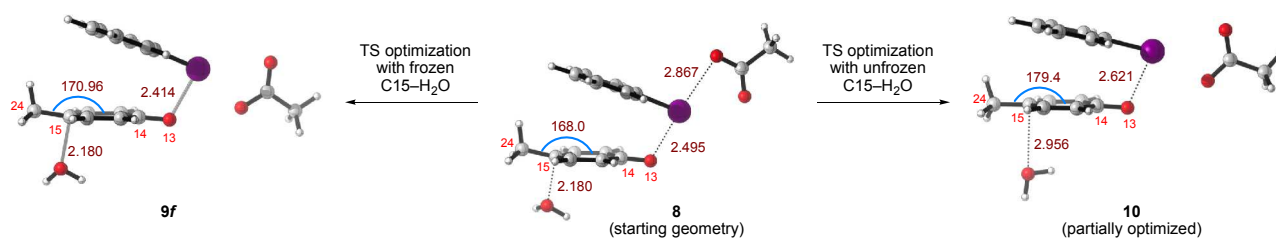
Figure 3. Attempt at identifying **TS3** by forcing the addition of H_2O to C15. Calculations performed only with a CH_3CN solvation model. The indicated atomic distances are in angstroms. The indicated bond angles are in degrees.

in **TS1** being close to the optimal distance (~3.5 Å) for π-π interactions[21] reinforces this idea. Similar intramolecular aryl-aryl interactions have been observed in the solid state with (arylsulfonylimino)iodoarenes (ArINSO$_2$Ar).[22]

In order to confirm that the calculated structure of **TS1** corresponds to the desired reaction, and not dissociation of phenoxide from **3**, the partial charges of several relevant species were evaluated. Details of this analysis can be found in the ESI and the results are summarized in Figure 2 (box). Summation of the Mulliken charges for the phenolic portion[5] (O13, C14–C19, C24) of λ³-iodane **3** resulted in a partial charge of approximately −0.45; indicating that this portion of **3** is best described as phenoxide-like. The acetate portion of **3** had a partial charge of about −0.59. Performing this analysis on **TS1** revealed a partial charge of approximately +0.35 for the phenolic portion and −0.92 for the acetate. An IRC calculation was attempted using **TS1** as a starting point, but this failed to complete and finished after only one or two steps. This failure may be due to a very flat potential energy surface.[23] A solution to this was realized by following the vibrational frequency of **TS1** in order to generate a new structure.[24] Optimization of this structure, with frozen† I–O13 and I–O30 distances, gave **7f**, which was found to be 1.3–3.7 kcal/mol lower in energy than **TS1**. The phenolic and acetate portions of **7f** had partial charges of +0.60–0.70 and −0.96, respectively. It is clear from this analysis that **TS1** does indeed represent the transition state for the direct fragmentation of λ³-iodane **3**.

Investigating the bimolecular decomposition pathway

Numerous attempts were made at locating a transition state structure corresponding to **TS3** (i.e., the direct addition of water to λ³-iodane **3**). Examples of these initial guesses include: microsolvation of the potential structure at the *para*-position of the phenolic portion of **3** (i.e., positioning a water molecule a suitable distance, <2.3Å, from C15), incorporating a water molecule into **TS1**, and incorporating the appropriate measurements of **TS2** into both **TS1** and **3**. None of these attempts lead to C–O bond formation in the transition state structure. Many resulted in the migration of the water molecule to non-productive distances (>3.0 Å from C15).

One set of experiments is illustrative of the problems we experienced and are the closest we have come to locating **TS3** (Figure 3). First, a guess structure (**8**) was constructed with the C15–O$_{H2O}$ distance frozen at 2.180 Å (a little shorter than the bond that is being made in **TS2**). Optimization to a transition state led to structure **9f**, wherein, the acetate had rotated to a position reminiscent of that in **TS1**. It was found that the C14–C15–C24 angle (170.96°) had not progressed toward the 165° angle found in **TS2** and was actually larger than that in the starting structure. Frequency analysis of structure **9f** revealed the presence of three imaginary frequencies. Two were found
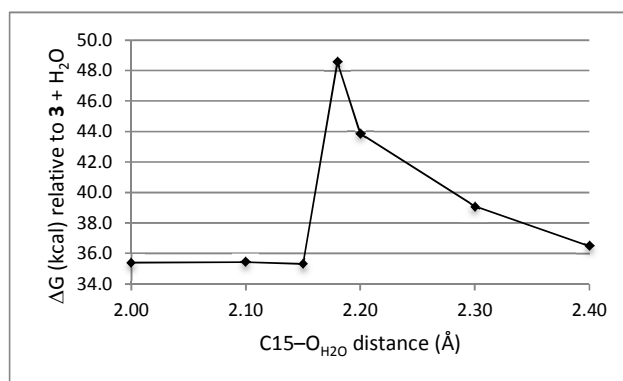

Figure 4. Free energy change (kcal/mol) as a function of C15–O$_{H2O}$ distance.

to be rocking motions involving the phenolic ring. The third was more interesting and appeared to represent the simultaneous breaking of the I–O13 bond and formation of the C15–O$_{H2O}$ bond (i.e. **TS3**).

Next, guess structure **8** was submitted for optimization to a transition state without a frozen C15–O$_{H2O}$ distance. One round of optimization gave rise to structure **10**. This partially converged structure closely resembled **TS1** with regard to the positioning of the aryl iodide, phenolic, and acetate portions. The C14–C15–C24 angle become more planar (179.4°) and the C15–O$_{H2O}$ distance increased to ~2.9 Å. The water molecule in **10** was also rotated in such a way that the oxygen lone pairs were no longer in a bond-making position. Interestingly, when structure **9f** was used as a starting point and optimized to a transition state with the C15–O$_{H2O}$ distance released from its constraint, a partially optimized structure was obtained that was highly reminiscent of structure **10** (I–O13: 2.628 Å; C15–O$_{H2O}$: 3.034 Å; C14–C15–C24: 178.9°). In other words, *the water was ejected from structure **9f** once the restriction was removed.*

Structure **9f** was then used as a starting point for a series of calculations in which the C15–O$_{H2O}$ distance was frozen at different distances and optimized. The free energy of these structures, relative to **3** + H_2O, are plotted as a function of C–O distance in Figure 4. As can be seen, the energy of the system steadily increases as the C–O distance decreases and reaches a maximum at 2.18 Å (structure **9f**). At distances of 2.20–2.40 Å, any imaginary frequencies corresponded to rocking motions or bond rotations. At distances of 2.00–2.15 Å, the I–O13 bond was completely broken (~3.5 Å) and any imaginary frequencies corresponded only to formation of the C15–O$_{H2O}$ bond (i.e., **TS2** with PhI and acetate present). It is important to note that all of these structures were higher in energy than **TS1**, and

structure **9f** (2.18 Å) was found to be 18 kcal/mol higher in energy than **TS1**.

Revisiting the barrier height of the unimolecular decomposition pathway

Finally, we decided to reinvestigate the 30 kcal/mol barrier required to reach **TS1**, as this seemed too high for a reaction that readily occurs at room temperature. We speculated that inaccurate handling of the developing charge separation in **TS1** and the modelling of acetate as a discrete species may be, at least partially, responsible for this large energy barrier.[25] At the same time, we recognized that the reaction medium will become increasingly acidic as the reaction progresses. One equivalent of acetic acid is produced during the initial ligand exchange between $PhI(O_2CCH_3)_2$ and the phenol. Another equivalent will be produced during the conversion of iodane **3** into dienone **6**. This led us to hypothesize that protonation of the acetate portion of iodane **3** (or hydrogen bonding to a protic solvent/reactant[26]) might lower the energetic cost of **TS1**. This would be similar to the use of Lewis and Brønsted acids to activate $PhI(O_2CCH_3)_2$ in order to carry out certain reactions.[27]
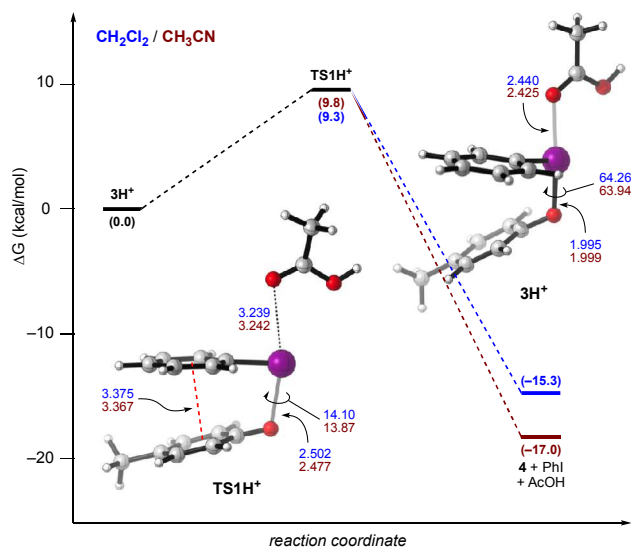

Figure 5. Energy profile for the redox decompostiont of **3H$^+$** using a CH_2Cl_2 (blue) or CH_3CN (maroon) solvation model. The numbers in parentheses are relative free energies (kcal/mol) for the listed compounds. All computed structures shown are with CH_3CN solvation. Structures in CH_2Cl_2 can be found in the supporting information. The indicated centroid and atomic distances are in angstroms. The indicated dihedral angles are in degrees.

To this end, the structures of protonated iodane **3** and transition state **TS1** were calculated (Figure 5). Protonation of the starting iodane (**3H$^+$**) causes lengthening the I–OAc bond by ~0.3 Å and shortening of the I–O$_{phenol}$ bond by almost 0.1 Å. The partial charge of the phenolate portion of iodane **3H$^+$** was also found to be overall negative (see ESI, Table S3). Gratifyingly, the protonated transition state (**TS1H$^+$**) was located with a barrier of about 10 kcal/mol. Interestingly, the leaving AcOH appears to follow a trajectory closer in line with the T-shape geometry of the iodane, rather than the dramatic rotation seen in **TS1**. This provides further evidence that the

rotation of the acetate in order to reach **TS1** serves to stabilize the developing negative charge through halogen bonding. The I–O$_{phenol}$ distance in **TS1H$^+$** was also about 0.3 Å shorter than then corresponding distance in **TS1**; befitting an earlier transition state. It is also interesting to note that the redox decomposition of **3H$^+$** to give phenoxenium **4** is exergonic by 15–17 kcal/mol. This makes sense when one considers that phenoxenium ions, albeit short lived, can be prepared and detected by other means.[7]

To be sure, structures **3H$^+$** and **TS1H$^+$** likely represent one end of a reactivity continuum, with structures **3** and **TS1** at the other end. The "true" structures would be somewhere in between, and are probably best described by a hydrogen-bonded network involving some combination of water, acetic acid, and acetate. Adequate modelling of this would require using explicit solvation and significantly higher computing cost. In order to do this properly, one needs to have known energies against which different structural models can be benchmarked.[28] Because experimental activation energies for iodine(III)-mediated dearomatization reactions have not been reported, any efforts at incorporating explicit solvent molecules would be entirely speculative.

Conclusions

Our work has, for the first time, shed some light on the nature of phenol oxidation by iodine(III) reagents and external nucleophiles. Taken as a whole, these results strongly suggest that the reaction of **3** with water proceeds through a phenoxenium ion (via **TS1**) rather than the direct addition of the nucleophile to the iodine(III) phenoxide (via **TS3**). This implies that a positive charge needs to be generated on the phenolic ring in order for it to be susceptible to nucleophilic attack. This makes sense when one considers that **TS3** requires a nucleophile (in this case water) to attack an "electrophile" (phenolic portion of **3** and **3H$^+$**) with an overall negative charge. However, the partial charge on the phenolic moiety, and C15 in particular, becomes more positive upon moving from **3→TS1→7f→4** (see ESI). Given that the aryl-λ^3-iodanyl group is considered to be a hypernucleofuge[29] with the ability to provide access to highly unstable species, like vinyl cations,[29,30] it is reasonable to conclude that an intermediate like **3** (or **3H+**) is perfect for realizing a direct two-electron oxidation of an aromatic ring to give an unstable[6,7] phenoxenium cation that will be trapped rapidly by the nucleophile.

Current research efforts are aimed at exploring how structural changes to both the phenol and the aryl iodide influence the relative energy of **TS1**. We are also using the results of this computational study as a basis for designing mechanistic experiments to confirm these computational results.

Acknowledgements

Conflicts of interest

There are no conflicts to declare.

Experimental

General computational details. Calculations were performed using the *Gaussian 09* suite[31] of electronic structure programs. All geometries were fully optimized at the M06-2X level[32] of density functional theory.[33] The 6–31+G(d) basis set[34] was used for C, H, and O. For iodine, the LANL2DZdp basis set[35] was used. An ultrafine grid density was used for numerical integration.[36] Unless otherwise noted, optimizations were performed with no frozen coordinates. Energy minima and transition states were identified though frequency analysis. The Gibbs energies (calculated for T = 298.15 K and 1 atm) for all relevant species can be found in Table S1. In order to account for solvation effects, the SMD solvation model[37] for CH_2Cl_2 and CH_3CN was employed during geometry optimizations. Graphics were generated using CYLview, 1.0b.[38]

Method used to generate structure 7f. Structure **7f** was generated as follows. **TS1** was opened in GaussView and the vibrations visualized. The single negative frequency (-109.1 in CH_3CN; -62.97 in CH_2Cl_2) was selected. Using the manual displacement slider, the displacement along this mode was set such that the oxygen atom of the phenolic group and the iodine atom were at a maximum displacement. This new structure was then saved and used as a starting point for a new optimization. Before optimizing this new structure, the I–O13 and I–O30 (one of the acetate oxygen atoms) distances were frozen. Freezing these distances ensures that the starting structure will be optimized to a structure on the reaction coordinate that is close to the transition state and will not fall to a local minimum.

Notes and references

† Structures calculated with a frozen coordinate are noted by *f*.

1   (a) *Hypervalent Iodine Chemistry: Modern Developments in Organic Synthesis*; T. Wirth, Ed.; Springer: Berlin, 2003. (b) V. V. Zhdankin *Hypervalent Iodine Chemistry*; Wiley: West Sussex, 2014.

2   (a) A. Pelter and R. S. Ward, *Tetrahedron* 2001, **57**, 273. (b) R. M. Moriarty and O. Prakash, *Org. React.* 2001, **57**, 327.

3   See Reference 1a, pp 8–11 and Reference 1b, pp 13–14.

4   (a) Y. Tamura, T. Yakura, J.-i. Haruta, Y. Kita, *J. Org. Chem.* 1987, **52**, 3927. (b) J. S. Swenton, A. Callinan, Y. Chen, J. J. Rohde, M. L. Kerns, and G. W. Morrow, *J. Org. Chem.* 1996, **61**, 1267. (c) A. Pelter, A. Hussain, G. Smith, and R. S. Ward, *Tetrahedron* 1997, **53**, 3879. (d) Y. Kita, M. Arisawa, M. Gyoten, M. Nakajima, R. Hamada, H. Tohma, and T. Takada, *J. Org. Chem.* 1998, **63**, 6625.

5   Frontier molecular orbital analysis of phenols has been used to support the formation of phenoxenium ions. See: L. Kürti, P. Herczegh, J. Visy, M. Simonyi, S. Antus, and A. Pelter, *J. Chem. Soc., Perkin Trans. 1* 1999, 379.

6   P. J. Hanway, and A. H. Winter, *J. Am. Chem. Soc.* 2011, **133**, 5086.

7   (a) P. J. Hanway, J. Xue, U. Bhattacharjee, M. J. Milot, Z. Ruixue, D. L. Phillips, and A. H. Winter, A. H. *J. Am. Chem. Soc.* 2013, **135**, 9078. (b) Y.-T. Wang, K. J. Jin, S. H. Leopold, J. Wang, H.-L. Peng, M. S. Platz, J. Xue, D. L. Phillips, S. A. Glover, and M. Novak, *J. Am. Chem. Soc.* 2008, **130**, 16021, and references therein.

8   A. M. Harned, *Tetrahedron Lett.*, 2014, **55**, 4681.

9   Recent reviews: (a) A. Parra, and S. Reboredo, *Chem. Eur. J.* 2013, **19**, 17244. (b) F. Singh, and T. Wirth, *Chem. Asian J.* 2014, **9**, 950. (c) F. Berthiol, *Synthesis* 2015, **47**, 587.

10 Recent examples: (a) S. J. Murray, and H. Ibrahim, *Chem. Commun.* 2015, **51**, 2376. (b) D.-Y. Zhang, L. Xu, H. Wu, and L.-Z. Gong, *Chem.—Eur. J.* 2015, **21**, 10314. (c) R. Coffinier, M. El Assal, P. A. Peixoto, C. Bosset, K. Miqueu, J.-M. Sotiropoulos, L. Pouységu, and S. Quideau, *Org. Lett.* 2016, **18**, 1120. (d) K. Antien, G. Viault, L. Pouységu, P. A. Peixoto, and S. Quideau, *Tetrahedron* 2017, **73**, 3684. (e) M. Ogasawara, H. Sasa, H. Hu, Y. Amano, H. Nakajima, N. Takenaga, K. Nakajima, Y. Kita, T. Takahashi, and T. Dohi, *Org. Lett.* 2017, **19**, 4102. (f) M. Uyanik, N. Sasakura, M. Mizuno, and K. Ishihara, *ACS Catal.* 2017, **7**, 872.

11 For a review of computational work involving hypervalent iodine mechanisms, see: A. Sreenithya, K. Surya, and R. B. Sunoj, *WIREs Comput. Mol. Sci.* 2017, **7**, e1299 (DOI: 10.1002/wcms.1299).

12 (a) Y. Kita, H. Tohma, K. Hatanaka, T. Takada, S. Fujita, S. Mitoh, H. Sakurai, and S. Oka, *J. Am. Chem. Soc.* 1994, **116**, 3684. (b) H. Tohma, H. Morioka, S. Takizawa, M. Arisawa, and Y. Kita, *Tetrahedron* 2001, **57**, 345. (c) T. Dohi, M. Ito, N. Yamaoka, K. Morimoto, H. Fujioka, and Y. Kita, *Tetrahedron* 2009, **65**, 10797.

13 Compare the results in: (a) A. W. Burgett, Q. L., Q. Wei, and P. G. Harran, *Angew. Chem. Int. Ed.* 2003, **42**, 4961. (b) H. Ding, P. L. DeRoy, C. Perreault, A. Larivée, A. Siddiqui, C. G. Caldwell, S. Harran, and P. G. Harran, *Angew. Chem. Int. Ed.* 2015, **54**, 4818.

14 (a) M. M. Kreevoy, and C. A. Mead, *J. Am. Chem. Soc.* 1962, **84**, 4596. (b) W. A. Alves, C. A. Téllez S, O. Sala, P. S. Santos, and R. B. Faria, *J. Raman Spectrosc.* 2001, **32**, 1032.

15 T. Clark, M. Hennemann, J. S. Murray, and P. Politzer, *J. Mol. Model.* 2007, **13**, 291.

16 (a) G. Cavallo, P. Metrangolo, R. Milani, T. Pilati, A. Priimagi, G. Resnati, and G. Terraneo, *Chem. Rev.* 2016, **116**, 2478. (b) C.-H. Tan, and C. W. Kee, Halogen Bond Catalysis: An Emerging Paradigm in Organocatalysis, *Nonnitrogenous Organocatalysis*; A. M. Harned, Ed.; CRC Press: Boca Raton, FL, 2018, pp 69–90.

17 The structure of Ph–I•OAc was only calculated in CH_3CN.

18 E. V. Anslyn, and D. A. Dougherty, *Modern Physical Organic Chemistry*; University Science Books: Sausalito, CA, 2006, pp 181–184.

19 (a) S. Grimme, *Angew. Chem. Int. Ed.* 2008, **47**, 3430. (b) K. K. Baldridge, F. Cozzi, and J. S. Siegel, *Angew. Chem. Int. Ed.* 2012, **51**, 2903.

20 J. C. Ma, and D. A. Dougherty, *Chem. Rev.* 1997, **97**, 1303.

21 M. O. Sinnokrot, and C. D. Sherrill, *J. Phys. Chem. A* 2006, **110**, 10656.

22 M. Boucher, D. Macikenas, T. Ren, and J. D. Protasiewicz, *J. Am. Chem. Soc.* 1997, **119**, 9366.

23 S. Koseki, and M. S. Gordon, *J. Phys. Chem.* 1989, **93**, 118.

24 Similar constrained optimizations have been used to approximate the IRC. See: D. V. Sadasivam, E. Prasad, R. A. Flowers, II, and D. M. Birney, *J. Phys. Chem. A* 2006, **110**, 1288.

25 For a discussion of the issues that must be considered in order to predict accurate energies of charged species, see: J. H. Jensen, *Phys. Chem. Chem. Phys.* 2015, **17**, 12441.

26 Houk has found that incorporating an explicit water molecule can alter transition state energies by about 10 kcal/mol. Y. Takano, and K. N. Houk, *J. Chem. Theory Comput.* 2005, **1**, 70.

27 For example: (a) Y.-B. Kang, and L. H. Gade, *J. Am. Chem. Soc.* 2011, **133**, 3658. (b) N. G. Moon, and A. M. Harned, *Tetrahedron Lett.* 2013, **54**, 2960. (c) S. Izquierdo, S. Essafi, I. del Rosal, P. Vidossich, R. Pleixats, A. Vallribera, G. Ujaque, A. Lledós, and A. Shafir, *J. Am. Chem. Soc.* 2016, **138**, 12747, and references therein.

28 For examples discussin proper solvation of carboxylates, see: (a) S. M. Bachrach, *J. Phys. Chem. A* 2008, **112**, 3722. (b) C. C. R. Sutton, G. V. Franks, and G. da Silva, *J. Phys. Chem. B* 2012, **116**, 11999. (c) C. C. Trout, and J. D. Kubicki, *Geochim. Cosmochim. Acta* 2006, **70**, 44.

29 Leaving group ability is five orders of magnitude greater than triflate. See: T. Okuyama, T. Takino, T. Sueda, and M. Ochiai, *J. Am. Chem. Soc.* 1995, **117**, 3360.

30 M. Ochiai, Y. Takaoka, K. Sumi, and Y. Nagao, *J. Chem. Soc., Chem. Commun.* 1986, 1382.

31 M. J. Frisch, G. W. Trucks, H. B. Schlegel, G. E. Scuseria, M. A. Robb, J. R. Cheeseman, G. Scalmani, V. Barone, B. Mennucci, G. A. Petersson, H. Nakatsuji, M. Caricato, X. Li, H. P. Hratchian, A. F. Izmaylov, J. Bloino, G. Zheng, J. L. Sonnenberg, M. Hada, M. Ehara, K. Toyota, R. Fukuda, J. Hasegawa, M. Ishida, T. Nakajima, Y. Honda, O. Kitao, H. Nakai, T. Vreven, J. A. Montgomery, Jr., J. E. Peralta, F. Ogliaro, M. Bearpark, J. J. Heyd, E. Brothers, K. N. Kudin, V. N. Staroverov, T. Keith, R. Kobayashi, J. Normand, K. Raghavachari, A. Rendell, J. C. Burant, S. S. Iyengar, J. Tomasi, M. Cossi, N. Rega, J. M. Millam, M. Klene, J. E. Knox, J. B. Cross, V. Bakken, C. Adamo, J. Jaramillo, R. Gomperts, R. E. Stratmann, O. Yazyev, A. J. Austin, R. Cammi, C. Pomelli, J. W. Ochterski, R. L. Martin, K. Morokuma, V. G. Zakrzewski, G. A. Voth, P. Salvador, J. J. Dannenberg, S. Dapprich, A. D. Daniels, O. Farkas, J. B. Foresman, J. V. Ortiz, J. Cioslowski, and D. J. Fox, *Gaussian 09*, Revision D.01; Gaussian, Inc.: Wallingford, CT, 2013.

32 Y Zhao, and D. G. Truhlar, *Theor. Chem. Acc.* 2008, **120**, 215.

33 C. J. Cramer, *Essentials of Computational Chemistry: Theories and Models*, 2nd ed.; Wiley: West Sussex, 2004.

34 W. J. Hehre, L. Radom, P. v. R. Schleyer, and J. A. Pople, *Ab Initio Molecular Orbital Theory*; Wiley: New York, 1986.

35 C. E. Check, T. O. Faust, J. M. Bailey, B. J. Wright, T. M. Gilbert, and L. S. Sunderlin, *J. Phys. Chem. A* 2001, **105**, 8111.

36 S. E. Wheeler, and K. N. Houk, *J. Chem. Theory Comput.* 2010, **6**, 395.

37 A. V. Marenich, C. J. Cramer, and D. G. Truhlar, *J. Phys. Chem. B* 2009, **113**, 6378.

38 C. Y. Legault, *CYLview*, Version 1.0b; Université de Sherbrooke, 2009 (http://www.cylview.org).